Available online at www.sciencedirect.com
SCIENCE DIRECT
Science Press
Trans. Nonferrous Met. Soc. China 16(2006) 122−126
Transactions of Nonferrous Metals Society of China
www.csu.edu.cn/ysxb/

Influence of annealing treatment on structural and magnetic properties of double perovskite Sr_2FeMoO_6

FENG Xiao-mei(冯晓梅)[1], LIU Guang-yao(刘广耀)[2], HUANG Qing-zhen(黄清镇)[3], RAO Guang-hui(饶光辉)[2]

1. College of Materials Science and Technology, Nanjing University of Aeronautics and Astronautics, Nanjing 210016, China;
2. Beijing National Laboratory for Condensed Matter Physics, Institute of Physics, Chinese Academy of Sciences, Beijing 100080, China;
3. NIST Center for Neutron Research, National Institute of Standards and Technology, Gaithersburg, MA 20899, USA

Received 5 July 2005; accepted 1 November 2005

Abstract: The structure, magnetic and electric properties of Sr_2FeMoO_6 (the as-made sample) and samples after heat treatment were investigated. The nuclear and magnetic structures of the samples were studied using neutron powder diffraction at room temperature. The results show that the tunneling magnetoresistance of polycrystalline Sr_2FeMoO_6 depends on its annealing temperature. Annealing at 800 ℃ makes the minimal magnetoresistance(MR) elevated, which may be due to the change of the grain size or the modified intergranular connections. Because of the impurity phase of Fe which probably affects the magnetotransport properties is much larger in sample C, so the MR is decreased by postannealing at 1100 ℃. Therefore, further enhancement of the tunneling magnetoresistance (TMR) can be realized by regulating the grain size at appropriate annealing temperature.

Key words: Sr_2FeMoO_6; double perovskite; neutron powder diffraction; magnetoresistance

1 Introduction

Recently, much interest has been focused on the magnetotransport properties of the half-metallic double perovskite Sr_2FeMoO_6 because of its tunneling magnetoresistance(TMR) at room temperature[1]. Sr_2FeMoO_6 is an ordered double perovskite of the $A_2BB'O_6$ type with Fe and Mo atoms alternating on the B and B' sites, respectively. In a simple picture, the ferrimagnetic structure can be described as an ordered array of parallel Fe^{3+} (S=5/2) magnetic moments, antiferromagnetically coupled with Mo^{5+} (S=1/2) spins. The fact that single crystal samples of Sr_2FeMoO_6 shows minimal magnetoresistance(MR) effect, contrary to the case of polycrystalline samples, indicates the importance of grain boundary effect in prototypical intergrain tunneling magnetoresistance (IMR)[2]. It has been demonstrated that the smaller the grain size is, the larger the IMR of polycrystalline Sr_2FeMoO_6 is [3, 4]. It is well known that the grain size and the grain boundary could be regulated by heat treatment. For Ba_2FeMoO_6, annealing at 1 273 K in H_2/Ar leads to a large increase of the resistivity compared with the as-synthesized material and the low field MR is significantly increased as well[5].

Therefore, the structure, magnetic and transport properties of Sr_2FeMoO_6 annealed at different temperatures were investigated. It was found that the saturation magnetization M_S, Curie temperature T_C and the magnitude of TMR are influenced obviously by the heat treatment. All these observations might be elucidated by the different annealing temperatures and the emergence of the second impurity phase.

2 Experimental

Polycrystalline Sr_2FeMoO_6 were prepared by solid-state reaction at high temperature. Stoichiometric amounts of $SrCO_3$, Fe_2O_3, and MoO_3 were mixed and calcined at 900 ℃ for 10 h in air. The calcined mixture was then finely pulverized and pressed into

Foundation item: Project(1998061304) supported by the National Natural Foundation of China
Corresponding author: FENG Xiao-mei; E-mail: fengxm@nuaa.edu.cn

pellets followed by sintering at 1 280 ℃ for 3 h in a stream of 5% H_2/Ar. The prototype samples (sample A) were then annealed for 6 h in the same atmosphere flow at 800 ℃ (sample B) and 1100 ℃ (sample C) respectively.

The initial characterization of the products was carried out on a Rigaku D/max 2500 diffractometer with Cu K_α radiation (50 kV, 250 mA) and a graphite monochrometer at room temperature. The degree of ordering of all samples was established by Rietveld analysis of the XRD patterns. All the neutron diffraction experiments were performed at NIST Center for Neutron Research (NCNR) on the high-resolution, 32-counter BT-1 diffractometer with a monochromatic neutron beam of wavelength 1.540 3 Å. Data were collected in the 2 θ range of 3°–166° with a step of 0.05°. The program Fullprof[6, 7] was used for the Rietveld refinement of the crystal and magnetic structures of the compound.

Field dependence of magnetization was measured at 4.2 K by a superconducting quantum interference device (SQUID) magnetometer. Temperature dependence of magnetization curves were measured by a vibrating sample magnetometer(VSM) in a field of 0.09 T. The Curie temperature was determined from the inflection point of the *M*—*T* curve. Transport properties were determined by the standard four-probe method using OXFORD MaglabExa measurement system.

3 Results and discussion

3.1 Neutron diffraction

All the patterns were refined by the Fullprof Rietveld refinement program. Typical NPD patterns for samples at room temperature are presented in Fig.1, in which the open circles stand for the observed intensities and the solid lines are the calculated patterns. The calculated patterns agree well with the experimental ones.

A pseudo-Voigt function were chosen to generate the line shape of the diffraction peaks. Two regions in the refinements were excluded (3°—15° and 158°—166°). In the final run the following parameters were refined based on the NPD data: scale factor, background coefficients, zero-point error, pseudo-Voigt parameters, together with the lattice parameters, oxygen atomic positions, isotropic temperature factors and the ordered magnetic moments of Fe and Mo. The coherent scattering lengths for Sr, Fe, Mo, and O were 7.02, 9.45, 6.72, and 5.803 fm, respectively. All the samples are essentially single phase with minor impurity phase of Fe, seen in the NPD patterns (0.39%, 0.31%, 1.16% for the samples A, B, and C, respectively). Its structure was

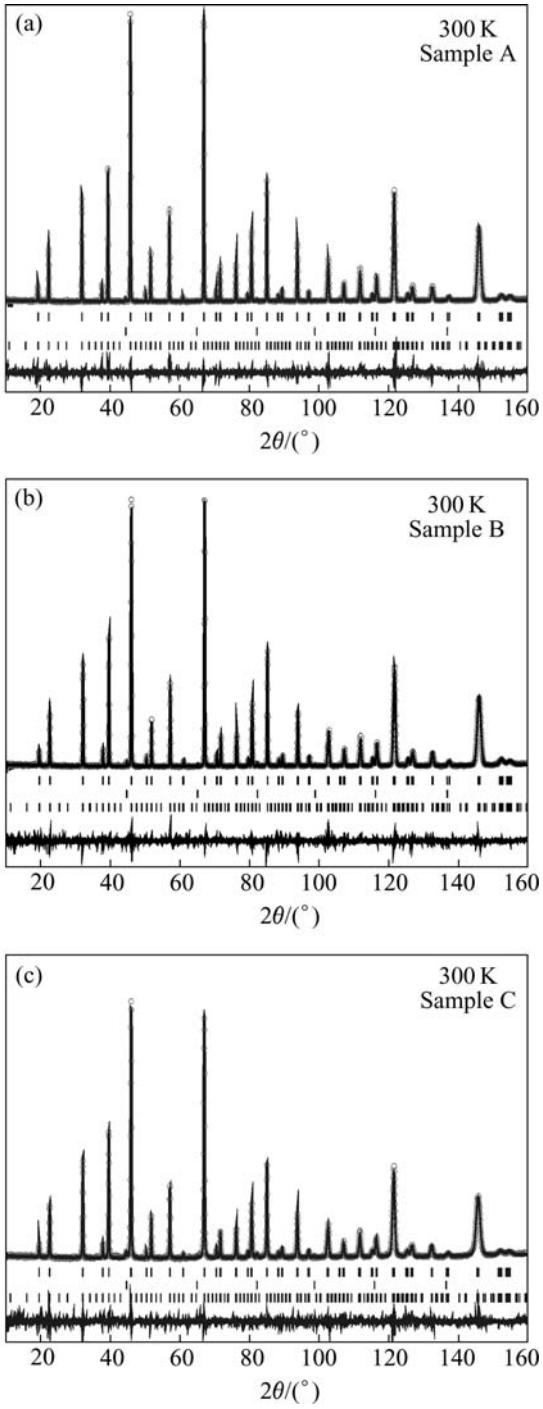

Fig.1 Experimental(open circles), calculated(full line) and difference(bottom) room-temperature NPD Rietveld profiles for samples (Bragg peaks, from high to low, correspond to nuclear Bragg reflections of Sr_2FeMoO_6, second phase of Fe, and magnetic Bragg reflections of Sr_2FeMoO_6)

included in the final refinements. At room temperature, all the samples have been fitted in the tetragonal I4/m symmetry with a constrain for O at (*x*, *y*, 0): *y*=1/2—*x*[8]. No significant difference in the fit is found either by using the $P4_2/m$ or the I4/mmm, in close agreement with those reported in Refs.[9, 10]. Refinement of site

occupancies could provide insight concerning what defects exist that could account for sample differences. In the Rietveld refinements with our data, the oxygen content is found to be "O_6" in trial refinements, and thus, the oxygen site occupancies were fixed at unity in the final refinements. The anti-site disordering obtained from the XRD patterns was included in the model, but it was not refined since a strong correlation with the magnetic contribution to the scattering was found in trial refinements. Refined structural parameters for samples B and C at room temperature are compared with those for sample A, listed in Table 1. The main interatomic distances for Sr_2FeMoO_6 are shown in Table 2. The *c*/*a* ratios (at 300 K), show a small increase of about 0.051% between samples A and B, and about 0.037% between samples A and C. Such a small structural differences suggest that any differences in chemical composition must be very subtle.

Since the perovskite unit cell is already doubled by the Fe/Mo ordering, all of magnetic reflections are coincident with nuclear Bragg reflections. From trial refinement, we found that unconstrained refinements based on four variables (the magnitudes and canting angles for the Fe and Mo ions) were too poorly determined to give a unique result. Thus, refinements of the magnetic structure were, first done by modeling a FM structure with magnetic moments only at the Fe positions, while fixing all parameters that affect nuclear Bragg intensities; a fixed orientation parallel to the *c* axis was considered. After the full refinement of the profile, the magnitude and the orientation of the Fe position were fixed. The subsequent introduction of magnetic moments at the Mo positions in an AFM arrangement with respect to Fe moments (i.e. describing a global ferrimagnetic structure) lead to a dramatic improvement of a discrepancy R_{mag} factors (Table 1). According to Ref.[11], the best fit was obtained with the spin direction parallel to the [110] direction, while in our refinement, the spatial orientation with the spin direction parallel to the [110] direction didn't led to any obvious improvement of the fit. We do not have sufficient sensitivity to say whether the Fe moments are canted as in Refs.[9, 11] at room temperature. After the final refinement, ordered moments on Fe and Mo at room temperature refined to $\mu_{Fe}=2.5(1)\mu_B$ and $\mu_{Mo}=-0.39(14)\mu_B$ for sample A, $\mu_{Fe}=2.40(9)\mu_B$ and $\mu_{Mo}=-0.44(12)\mu_B$ for sample B, $\mu_{Fe}=2.25(14)\mu_B$ and $\mu_{Mo}=-0.38(18)\mu_B$ for sample C. These values yield a total effective magnetic moment of about $2.11\mu_B$ for sample A, about $1.96\mu_B$ and about $1.87\mu_B$ for sample B and sample C, respectively.

Table 1 Structure and magnetic parameters after Rietveld refinement of NPD patterns for Sr_2FeMoO_6 at 300 K(samples A, B, and C)

Space group	I4/m		
	Sample A	Sample B	Sample C
a/Å	5.572 974(15)	5.572 598(13)	5.573 710(25)
c/Å	7.896 927(36)	7.900 429(31)	7.900 898(63)
c/*a*	1.417 00	1.417 73	1.417 53
Vol./Å^3	245.263(1)	245.339(1)	245.451(2)
B at (0 0 0): Occup.	$Fe_{0.90}Mo_{0.10}$	$Fe_{0.89}Mn_{0.11}$	$Fe_{0.87}Mo_{0.13}$
B/Å^2	0.38(3)	0.42(4)	0.84(7)
Magnetic moment(μ_B)	2.5(1)	2.40(9)	2.25(14)
B′ at (0 0 1/2): Occup.	$Mn_{0.90}Fe_{0.10}$	$Mo_{0.89}Fe_{0.11}$	$Mo_{0.87}Fe_{0.13}$
B/Å^2	0.32(5)	0.25(5)	−0.001(80)
Magnetic moment(μ_B)	−0.39(14)	−0.44(12)	−0.38(18)
Sr at (1/2 0 1/4)			
B/Å^2	0.73(4)	0.771(3)	0.877(5)
O(1) at (0 0 *z*)			
z	0.253 72(38)	0.253 17(39)	0.251 72(75)
B/Å^2	0.71(1)	0.83(1)	0.77(2)
O(2) at (*x y* 0)			
x	0.266 81(8)	0.268 27(7)	0.268 09(8)
y	0.233 19(8)	0.231 73(7)	0.231 91(8)
B/Å^2	1.052(8)	0.949(7)	1.11(1)
x^2	1.39	1.24	1.73
R_p/%	5.21	4.51	5.69
R_{wp}/%	6.47	5.84	7.33
R_{mag}/%	11.8	11.0	13.8

Table 2 Selected bond lengths for Sr_2FeMoO_6 at 300 K (samples A, B, and C)

Space group	I4/m		
	Sample A	Sample B	Sample C
Fe-O(1)×2	2.003(3)	2.000(3)	1.988(5)
Fe-O(2)×4	1.9747(6)	1.9754(5)	1.9757(6)
Mo-O(1)×2	1.944(3)	1.950(3)	1.961(5)
Mo-O(2)×4	1.9747(6)	1.9754(5)	1.9757(6)

3.2 Transport properties

The magnetization curves at 4.2 K in Fig.2 show that the saturation magnetization M_S decreases from 3.49μ_B/*f.u.* for sample A to 3.33μ_B/*f.u.* for sample B and 2.88μ_B/*f.u.* for sample C. The variational tendency of the magnetization for the three samples parallels to the refined magnetic moments of the three samples at room temperature. The low observed M_S values for this material have been explained by a Monte Carlo simulation taking into consideration of the disorder on the B-site[12, 13]. The anti-site occupancy of Mo at Fe positions and vice versa would give a variation of the saturation magnetization as M_S=(4−8 *AS*) μ_B /*f.u.*, where *AS* (anti-site) is the fraction of Fe atoms replaced by Mo. In our samples, the *AS* derived from the XRD Rietveld refinement results is 10% for sample A, 11% for sample B and 13% for sample C, respectively. The M_S evaluated from the above formula agrees reasonably with the experimental values. Postannealing does not improve much the ordering of Fe and Mo. This is different from Ref.[2] reporting that the Fe/Mo ordering was increased from 85% to 92% through annealing.

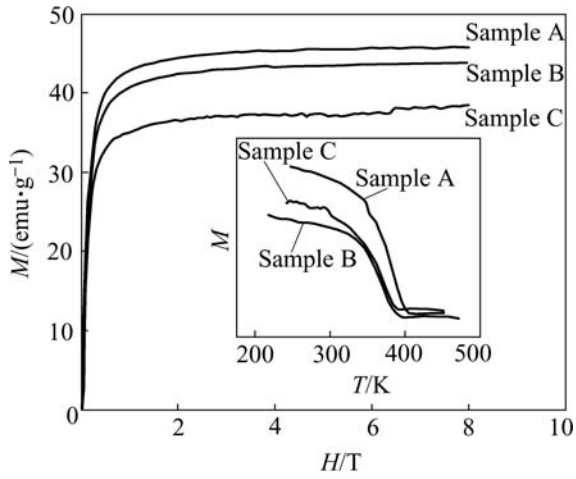

Fig.2 Magnetization curves of samples A, B, C at 4.2 K(Inset is temperature dependence of magnetization in a field of 0.09 T)

The temperature dependence of magnetization of the compounds is shown in the inset of Fig.2. The derived Curie temperature T_C decreases from 400 K for sample A to 388 K for sample B and 385 K for sample C.

The $\rho(T)$ curves registered under zero field reveal that all the samples exhibit a insulator-metal transition between 5 K and 300 K (Fig.3). This behavior could be a weak ANDERSON localization reduced by some disorder in the Fe and Mo sites[14]. The resistivities of the annealed samples are increased compared to the as-synthesized samples. Fig.4 displays a peak of the XRD pattern. We found that the FWHM (full width at half maximum) increases after annealing, which may indicates that the grain size decreases with the heat treatment. The decreasing of grain size leads to the more grain boundaries and to the increase of the resistivity.

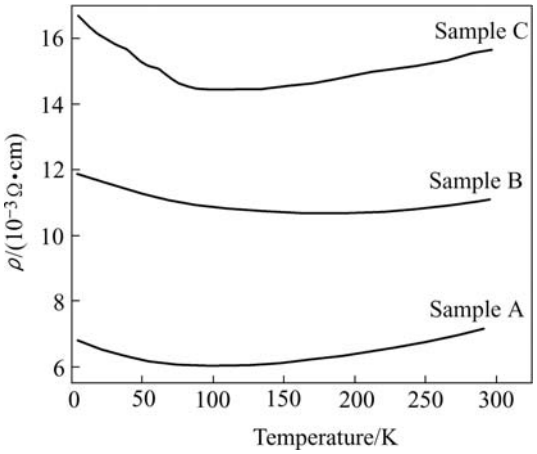

Fig.3 Resistivity under zero field as function of temperature

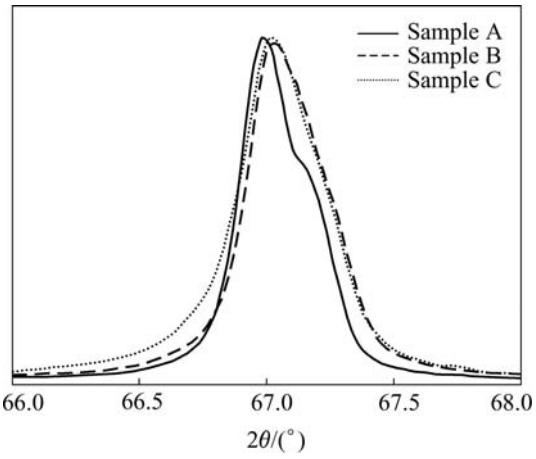

Fig.4 Comparison of peak profile (about 67°)

We define M_R={ρ(H)−ρ(0)}/ρ(0), where $\rho(H)$ is the resistivity in a magnetic field of *H*. From Fig.5, we found that the $|M_R|$ was elevated significantly after annealing at 800 ℃ for 6 h (sample B) while decreased again when annealing temperature raised up to 1 100 ℃ (sample C) at 270 K. In general, the more the grain boundaries are, the larger the TMR effects are. The grain boundaries work as potential barriers,

through which a TMR is realized. From the $\rho(T)$ curves and the FWHM, we concluded that the grain sizes of the annealed samples may be decreasing, which means more grain boundaries were introduced and the intergranular connections were modified, so the TMR elevated. This explanation is only applied to sample B but not to sample C. For sample C, the sharp decreasing of TMR may be attributed to the quantity of impurity phase of Fe which is about four times larger in sample C than in sample B. It is well established that the insulating barriers located at the grain boundaries strongly promote the TMR, but in our samples the ferromagnetic impurity phase probable affects the magnetotransport properties through disturbing the long-range order of Fe-O-Mo[15]. Another reason may be the larger anti-site concentration in sample C.

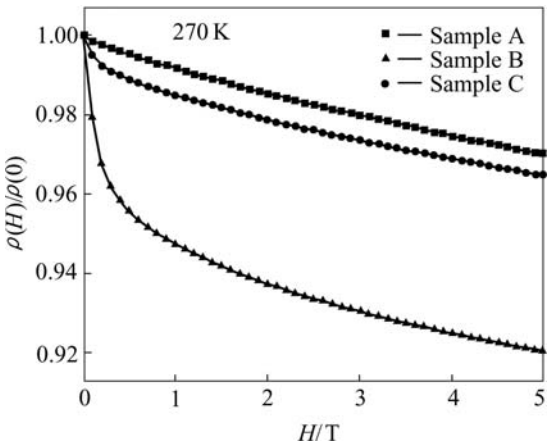

Fig.5 $\rho(H)/\rho(0)$ as function of applied field

4 Conclusions

The tunneling magnetoresistance of polycrystalline Sr_2FeMoO_6 depends on its annealing temperature. Annealing at 800 ℃ made the M_R elevated, which may be due to the intergranular connections were modified or the change of the grain size. Because of the impurity phase of Fe which probable affects the magnetotransport properties is much larger in sample C, so the M_R is decreased by postannealing at 1 100 ℃. Therefore, further enhancement of the TMR could be realized by regulating the grain size at appropriate annealing temperature.

References

[1] KOBAYASHI K I, KIMURA T, SAWADA H. Room-temperature magnetoresistance in an oxide material with an ordered double-perovskite structure[J]. Nature, 1998, 395: 677－680.

[2] TOMIOKA Y, OKUDA T, OKIMOTO Y, et al. Magnetic and electronic properties of a single crystal of ordered double perovskite Sr_2FeMoO_6[J]. Phys Rev B, 2000, 61: 422－427.

[3] YUAN C L, NANG S G, SONG W H, et al. Enhanced intergrain tunneling magnetoresistance in double perovskite Sr_2FeMoO_6 polycrystals with nanometer-scale particles[J]. Appl Phys Lett, 1999, 75: 3853－3855.

[4] YUAN C L, ZHU Y, ONG P P. Enhancement of room-temperature magnetoresistance in Sr_2FeMoO_6 by reducing its grain size and adjusting its tunnel-barrier thickness[J]. Appl Phys Lett, 2003, 82: 934－936.

[5] MAIGNAN A, RAVEAU B, MARTIN C, et al. Large intergrain magnetoresistance above room temperature in the double perovskite Ba_2FeMoO_6[J]. J Solid State Chem, 1999, 144: 224－227.

[6] RIETVELD H M. Line profiles of neutron powder-diffraction peaks for structure refinement[J]. Acta Cryst, 1969, 22: 151－152.

[7] YOUNG R A, WILES D B. Profile shape functions in rietveld refinements[J]. J Appl Cryst, 1982, 15: 430－438.

[8] BLASCO J, RITTER C, MORELLON L, et al. Structural, magnetic and transport properties of $Sr_2Fe_{1-x}Cr_xMoO_{6-y}$[J]. Solid State Sciences, 2002, 4: 651－660.

[9] CHMAISSEM O, KRUK R, DABROWSKI B, et al. Structural phase transition and the electronic and magnetic properties of Sr_2FeMoO_6[J]. Phys Rev B, 2000, 62: 14197－14206.

[10] SÁNCHEZ D, ALONSO J A, GARCÍA-HERNÁNDEZ M, et al. Origin of neutron magnetic scattering in antisite-disordered Sr_2FeMoO_6 double perovskites[J]. Phys Rev B, 2002, 65: 1044261－1044268.

[11] RITTER C, IBARRA M R, MORELLON L, et al. Structural and magnetic properties of double perovskites AA'$FeMoO_6$ (AA' = Ba_2, BaSr, Sr_2 and Ca_2)[J]. J Phys: Condens Matter, 2000, 12: 8295－8308.

[12] OGALE A S, OGALE S B, RAMESH R, et al. Octahedral cation site disorder effects on magnetization in double-perovskite Sr_2FeMoO_6: Monte Carlo simulation study[J]. Appl Phys Lett, 1999, 75: 537－539.

[13] BALCELLS L, NAVARRO J, BIBES M, et al. Cationic ordering control of magnetization in Sr_2FeMoO_6 double perovskite[J]. Appl Phys Lett, 2000, 78: 781－783.

[14] NIEBIESKIKWIAT D, SÁNCHEZ R D, CANEIRO A, et al. High-temperature properties of the Sr_2FeMoO_6 double perovskite: Electrical resistivity, magnetic susceptibility, and ESR[J]. Phys Rev B, 2000, 62: 3340－3345.

[15] NIEBIESKIKWIAT D, CANEIRO A, SÁNCHEZ R D, et al. Oxygen-induced grain boundary effects on magnetotransport properties of $Sr_2FeMoO_{6+\delta}$[J]. Phys Rev B, 2001, 64: 1804061－1804064.

(Edited by LI Xiang-qun)